


FULL ARTICLE

Multispectral optoacoustic tomography of muscle perfusion and oxygenation under arterial and venous occlusion: A human pilot study

Angelos Karlas^{1,2,3,5} | Michael Kallmayer³ | Nikolina-Alexia Fasoula^{1,2} |
 Evangelos Liapis^{1,2} | Michail Bariotakis^{1,2}  | Markus Krönke⁴ |
 Maria Anastasopoulou^{1,2} | Josefine Reber^{1,2} | Hans-Henning Eckstein^{3,5} |
 Vasilis Ntziachristos^{1,2,5*}

¹Chair for Biological Imaging, Center for Translational Cancer Research (TranslaTUM), Technical University of Munich, Munich, Germany

²Helmholtz Zentrum München, Institute of Biological and Medical Imaging, Neuherberg, Germany

³Clinic of Vascular and Endovascular Surgery, Technical University of Munich, Munich, Germany

⁴Clinic of Nuclear Medicine, Technical University of Munich, Klinikum Rechts der Isar, Germany

⁵DZHK (German Centre for Cardiovascular Research), Partner Site Munich Heart Alliance, Munich, Germany

*Correspondence

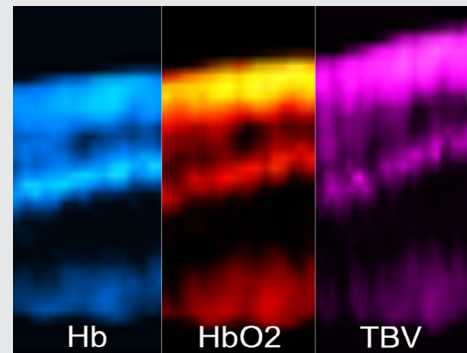
Vasilis Ntziachristos, Chair for Biological Imaging, Center for Translational Cancer Research (TranslaTUM), Technical University of Munich, Ismaninger Str. 22, 81675, Munich, Germany.
 Email: v.ntziachristos@gmail.com

Funding information

Bundesministerium für Bildung und Forschung; Deutsches Zentrum für Herz-Kreislaufforschung; Helmholtz Zentrum Muenchen, Grant/Award Number: Physician Scientists for Groundbreaking

Abstract

Perfusion and oxygenation are critical parameters of muscle metabolism in health and disease. They have been both the target of many studies, in particular using near-infrared spectroscopy (NIRS). However, difficulties with quantifying NIRS signals have limited a wide dissemination of the method to the



clinics. Our aim was to investigate whether clinical multispectral optoacoustic tomography (MSOT) could enable the label-free imaging of muscle perfusion and oxygenation under clinically relevant challenges: the arterial and venous occlusion. We employed a hybrid clinical MSOT/ultrasound system equipped with a hand-held scanning probe to visualize hemodynamic and oxygenation changes in skeletal muscle under arterial and venous occlusions. Four (N = 4) healthy volunteers were scanned over the forearm for both 3-minute occlusion challenges. MSOT-recorded pathophysiologically expected results during tests of disturbed blood flow with high resolution and without the need for contrast agents. During arterial occlusion, MSOT-extracted Hb-values showed an increase, while HbO₂- and total blood volume (TBV)-values remained roughly steady, followed by a discrete increase during the hyperemic period after cuff deflation. During venous occlusion, results showed a clear increase in intramuscular HbO₂, Hb and TBV within the segmented muscle area. MSOT was

Angelos Karlas and Michael Kallmayer contributed equally to the study.

This is an open access article under the terms of the Creative Commons Attribution-NonCommercial-NoDerivs License, which permits use and distribution in any medium, provided the original work is properly cited, the use is non-commercial and no modifications or adaptations are made.

© 2020 The Authors. *Journal of Biophotonics* published by WILEY-VCH Verlag GmbH & Co. KGaA, Weinheim

Projects; Horizon 2020 Framework Programme, Grant/Award Number: 694968

found to be capable of label-free non-invasive imaging of muscle hemodynamics and oxygenation under arterial and venous occlusion. We introduce herein MSOT as a novel modality for the assessment of vascular disorders characterized by disturbed blood flow, such as acute limb ischemia and venous thrombosis.

KEYWORDS

ischemia, muscle metabolism, peripheral arterial disease, photoacoustics, thrombosis

1 | INTRODUCTION

Muscle perfusion and oxygenation (MOx) are key components of muscle metabolism affected in several diseases, including peripheral arterial disease (PAD), deep vein thrombosis (DVT), heart failure and diabetes mellitus [1–5]. Non-invasive perfusion and MOx measurements are desirable for quantifying parameters associated with fitness level, disease severity and therapy efficacy. Traditional methods of measuring these parameters, such as the ultrasound, the magnetic resonance spectroscopy (MRS) and imaging (MRI), or nuclear medicine techniques (eg, positron emission tomography, PET) have limitations that impair direct testing of muscle function and their application to large-scale studies: they do not provide direct MOx information, are costly or employ ionizing radiation.

Near-infrared spectroscopy (NIRS) and diffuse optical tomography (DOT) have been investigated as techniques for high-throughput non-invasive and label-free assessment of MOx and muscle hemodynamics in real-time [6–8]. NIRS allows for direct sensing and differentiation of oxy- (HbO_2) and deoxy-hemoglobin (Hb) and was thus introduced as a technique for imaging hemodynamics and oxygen of soft tissues. Furthermore, NIRS reaches depths of several centimeters, due to the low attenuation of light at infrared wavelengths. While the HbO_2 - and Hb-contrast achieved by NIRS and DOT is indeed valuable for the assessment of metabolic function, there are significant limitations in the quantitative accuracy and the resolution achieved [9]. Their fundamental limit comes from the strong photon scattering in tissues, which generates uncertainty in the information collected. In fact, it is challenging to extract the individual contributions of Hb and HbO_2 from the measured scattering alterations in tissues and thus to achieve quantification of hemoglobin. Moreover, the techniques offer very low spatial resolution, mixing contributions from muscle and more superficial tissues, such as the fat and the skin. Until today, neither NIRS nor DOT have found widespread acceptance in the clinics [10, 11].

Optoacoustic imaging is a high-resolution method that solves the fundamental limitations of purely optical imaging by using ultrasonic instead of optical detection,

making it insensitive to photon scattering. The method has been employed to image peripheral arteries [12, 13], arteriovenous malformations [14], breast cancer [15], systemic sclerosis [16], Crohn's disease [17] or brown fat activation over time [18]. Optoacoustic imaging has also shown ability to perform monitoring of hemodynamic responses after exercise in healthy volunteers [19]. A next step with clinical relevance is to examine whether the method could image hemodynamics and oxygenation changes under conditions typical of blood flow disturbances, such as arterial and venous occlusion.

Our purpose was to investigate whether clinical optoacoustics, in particular multispectral optoacoustic tomography (MSOT), could enable the label-free imaging of muscle perfusion and oxygenation under conditions of arterial and venous occlusion, which simulate the acute limb ischemia and the venous thrombosis correspondingly.

2 | METHODS

2.1 | Study design and experimental protocol

All healthy volunteers consented to participate in the measurements in full accordance with the work safety regulations of the Helmholtz Center Munich (Neuherberg, Germany). All four ($N = 4$, 2 males, 2 females, age mean 36, range 33–37) subjects were non-smokers. They were asked to avoid consuming caffeine, food and alcohol for at least 8 hours before the planned measurements.

Tests took place in a dark, quiet room with an average temperature of $\sim 24^\circ\text{C}$ over the whole duration of the recordings. Subjects sat with their arms at heart-level. After 5 minutes of rest, the blood pressure of each subject was measured three times to confirm that all were normotensive. For the venous occlusion challenge, the cuff was inflated to a pressure of 80 mm Hg. For the arterial occlusion challenge, the cuff was inflated up to 40 mm Hg above the subject's systolic blood pressure (SBP), as extracted by the mean value of the three blood pressure readings. The MSOT probe was applied along the forearm and over the brachioradialis muscle

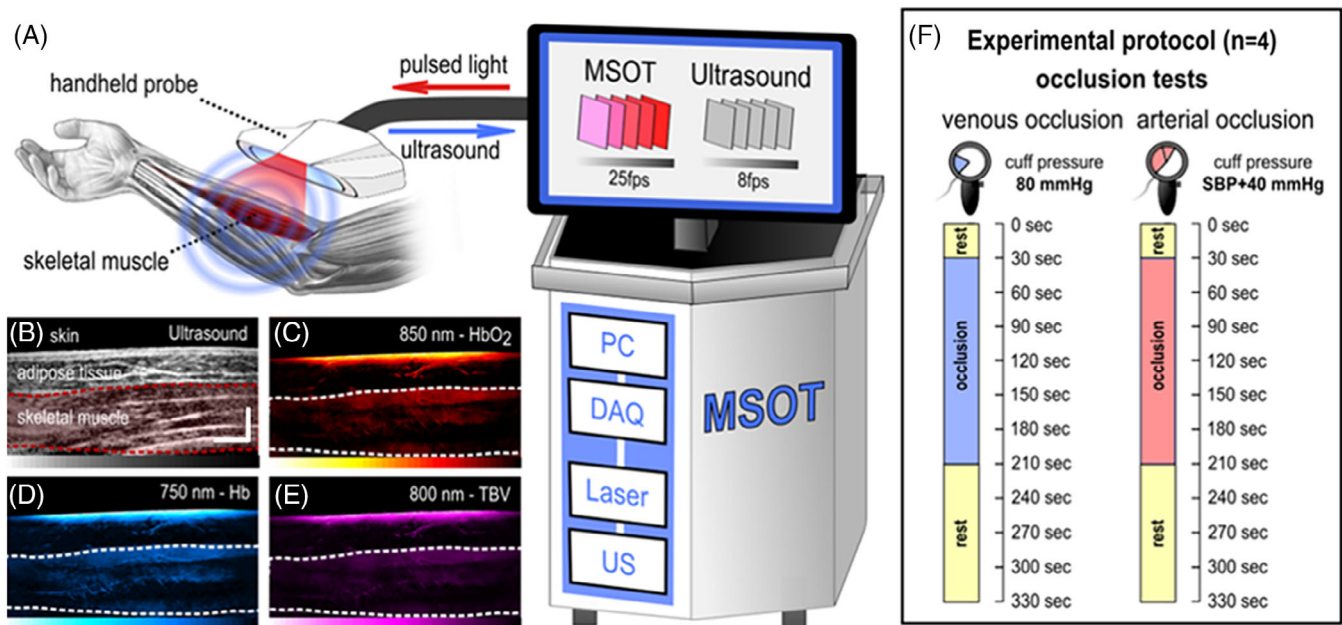


FIGURE 1 System principle of operation and experimental protocol. A, Hybrid clinical MSOT/ultrasound employs a handheld probe for real-time multispectral image acquisition of the skeletal muscles in the human forearm (wavelength range: 700–970 nm). B, Ultrasound image of the human forearm: The skin surface, the subcutaneous adipose tissue and the muscle regions (light red region) are tagged. Scale bars: 1 cm. MSOT image of the forearm region acquired (C) at 850 nm, where HbO₂ (oxygenated hemoglobin) light absorption is significantly higher compared to Hb (deoxygenated hemoglobin), D, at 750 nm, where Hb light absorption is significantly higher compared to HbO₂ and E, at 800 nm, where HbO₂ light absorption equals that of Hb (isobestic point which represents the TBV, total blood volume). The white dotted line marks the measured muscle area. F, The experimental protocol followed for the occlusion tests on the four participating subjects. DAQ, data acquisition card; Hb, deoxy-hemoglobin; HbO₂, oxy-hemoglobin; MSOT, multispectral optoacoustic tomography; SBP, systolic blood pressure; TBV, total blood volume

identified by anatomic knowledge and after activating it by handgrip contractions under real-time ultrasound imaging (Figure 1).

2.2 | Handheld multispectral optoacoustic imaging

Measurements were conducted using a hybrid clinical MSOT/ultrasound system (Acuity, iTheraMedical GmbH, Munich, Germany) equipped with a handheld scanning probe. The system was able to acquire real-time optoacoustic and ultrasound data simultaneously at a framerate of 25 Hz for the optoacoustic data and ~9 Hz for the ultrasound data. The casing of the handheld probe was three-dimensional (3D)-printed offering decreased weight and increased flexibility and freedom to the operator (Figure 1A). The water tank was filled with heavy water (D₂O) which is characterized by less light absorption at the near-infrared range, compared to the normal water, while providing ideal coupling of the ultrasound waves in tissue in response to light absorption. The handheld probe was equipped with 256 piezoelectric elements with a central frequency of 4 MHz arranged in an arc of

145° for ultrasound detection. Illumination was delivered to tissue through an optical fiber, which was mounted on the same hand-held probe. Illumination was delivered in the form of short light pulses (~10 ns in duration), at a rate of 25 Hz. For each pulse, almost 15 mJ of energy were delivered over a rectangle area of around 1 × 4 cm, which is far below the safety limits of laser use for medical applications [20]. For multispectral image acquisition, we employed 28 different light wavelengths (from 700 to 970 nm at steps of 10 nm). All acquired optoacoustic data were further reconstructed using a model-based reconstruction method published before [21].

2.3 | Image segmentation, analysis and visualization

Muscle segmentation was performed by means of a custom-made semi-automated algorithm based on active contours [22]. For each venous or arterial occlusion recording, a muscle ROI was manually delimited in a single image used for the initialization of the semi-automated algorithm. This was performed after building consensus between two clinicians with extensive

experience in clinical ultrasound and MSOT imaging. For each initialization image the muscle was first visually identified in the corresponding and co-registered ultrasound image, based on previous knowledge of the local anatomy and the characteristic texture of muscle in ultrasound. Then, a curved ROI was manually delineated directly on the initialization image: an addition of the optoacoustic image corresponding to the 800 nm, which represents the total blood volume (TBV), and the one corresponding to the 970 nm, which represents the water tissue content. This way we ensured that the decision of the two clinicians was based more on functional and physiological information, taking into account that the skeletal muscle is a highly perfused and hydrated tissue, and less on purely morphological information, provided by ultrasound. Manual segmentation of the muscle was repeated three times to ensure consistency of results, based on three different initialization images: one corresponding to the resting period before the occlusion, one corresponding to the occlusion period and one corresponding to the resting period after the end of occlusion. For each of the three readouts a value for the HbO₂-, Hb- or TBV-level for each MSOT frame was extracted by averaging the absorption values of all pixels within the muscle ROI for this frame. Thus, (a) The Hb-points were extracted from the sequence of the successive 750 nm-frames, (b) The TBV-signal were extracted from the successive 800 nm-frames and (c) the HbO₂-signal were extracted from the successive 850 nm frames. Finally, the mean value of the three readouts for each time point was plotted as the HbO₂-, Hb- or TBV-level for this time point. The per subject baseline value for each physiological parameter (Hb, HbO₂ or TBV) was calculated as the average of all the plotted values over the first 30 seconds of the recording before the inflation of the occlusion cuff.

The manual segmentation of the initialization image resulted in an initial binary image with the pixels belonging to the muscle ROI having non-zero intensity (white) and all other background pixels having zero intensity (black). Subsequently, a binary image was automatically calculated for each multispectral stack (28 recorded single-wavelength frames from 700 to 970 nm at steps of 10 nm) throughout each recording based on the binary image or muscle ROI corresponding to the previous one. The rules controlling the calculation of each binary image, or the muscle ROI from the previous image, were regulated by the principle of the active contours, which aims at minimizing the energy defined by the forces tending to expand the contour (imaged intensity-based) and the ones tending to shrink it (smoothing-based). Taking into account the absence of significant motion throughout the whole recording, the evolution of the active contour or muscle ROI was smooth. All calculations and

quantifications took place on the raw optoacoustic images. For visualization purposes, all images were denoised and lightly contrast-enhanced to the same extent.

3 | RESULTS

3.1 | Venous occlusion challenge

The venous occlusion challenge in human volunteers shows an increase of muscle Hb, HbO₂ and TBV during the occlusion due to the obstruction of the forearm venous outflow, while maintaining an arterial inflow. The maximum median Hb-increase from the baseline is observed at the 3rd or last minute of venous occlusion (+30.91% compared to baseline). After the cuff deflation, the Hb-signal shows a radical decrease of -21.44%, reaching a level of +9.47% compared to baseline, as demonstrated in the image series of Figure 2A. Accordingly, the maximum median increase of the HbO₂ (+27.54%) and TBV signal (+27.64%) over the scanned muscle, compared to the subject's baseline, are observed at the 2nd minute after cuff inflation. All measured optoacoustic signals return to roughly baseline levels after the end of venous occlusion. With reference to hemodynamics (TBV fluctuations) and dynamics of HbO₂ and Hb, an indicator of intramuscular oxygen kinetics, our median venous occlusion readouts showed the fluctuations presented in Table 1.

These trends are represented visually in Figure 2. Figure 2A depicts the MSOT image series of the Hb-distribution within the forearm muscle of Subject 3 for each minute of the venous occlusion challenge. All images correspond to the 750 nm light wavelength, where light absorption of Hb is critically higher than that of HbO₂. Figure 2B,C depicts the corresponding MSOT image series for the HbO₂- and TBV-distributions in the forearm muscle of the same subject. The HbO₂ images correspond to 850 nm, where HbO₂ light absorption is higher than that of Hb, and the TBV images to 800 nm light wavelength, which is the isosbestic point of Hb, and HbO₂, where the absorptions of the two hemoglobins are equal. The observable fluctuations in the images are in line with the quantitative measures of hemodynamics and oxygenation plotted in Figure 2D for Subject 3.

Figure 2E summarizes the statistics of the Hb-levels during the venous occlusion test for the whole group of participating subjects (n = 4). Correspondingly, the box plots of Figure 2F,G presents the statistics of the HbO₂- and TBV-levels during the venous occlusion challenge for all subjects. The marked median values for the sample represent the central trend of change in relation to the per-subject baseline. These are calculated from the four

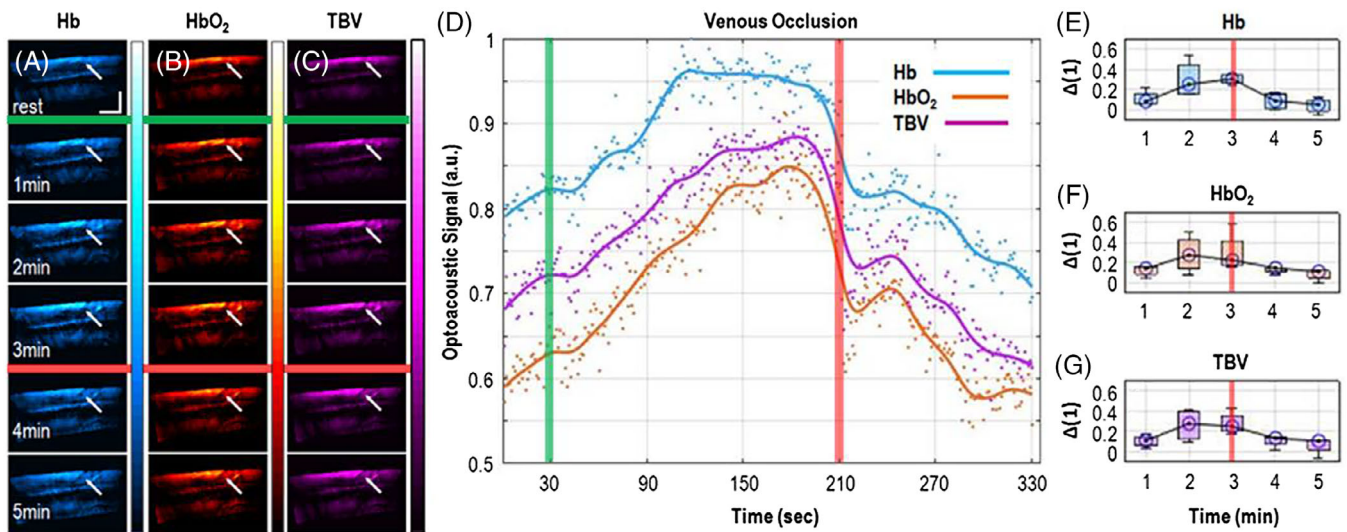


FIGURE 2 Multispectral optoacoustic tomography (MSOT) imaging of the forearm muscle hemodynamics and oxygen kinetics during venous occlusions. The whole process lasts 5.5 min: 0.5 min of baseline measurement, 3 min of cuff-induced venous occlusion and 2 min measurement after cuff deflation. Representative image series of A, Deoxy-hemoglobin (Hb)-distribution (MSOT at 750 nm), B, oxy-hemoglobin (HbO₂)-distribution (MSOT at 850 nm) and C, total blood volume (TBV)-distribution (MSOT at 800 nm) within the segmented muscle area at different time points of the venous occlusion challenge (Subject 3). The white arrows point to the muscle region where the changes are more prominent. Scale bars: 1 cm. D, Representative time plot (smoothing splines) of the mean optoacoustic signal for Hb, HbO₂ and TBV within the segmented muscle area over the whole venous occlusion challenge (Subject 1). Box plot of the mean change of E, Hb, F, HbO₂ and G, TBV optoacoustic signal within the muscle for each minute of the venous occlusion challenge, with regard to the corresponding baseline value for all (n = 4) subjects. The green thin stripe corresponds to the time point of cuff inflation. The red stripe corresponds to the time point of the cuff deflation

TABLE 1 Venous occlusion challenge: Total fluctuations of total blood volume (TBV), oxy- (HbO₂) and deoxy-hemoglobin (Hb) compared to the baseline, along with per-minute percentage changes (Δ) for all healthy volunteers

Time	TBV		HbO ₂		Hb	
	Δ (%)	Total (%)	Δ (%)	Total (%)	Δ (%)	Total (%)
First minute of occlusion	+11.11	+11.11	+14.32	+14.32	+8.69	+8.69
Second minute of occlusion	+16.53	+27.64	+13.22	+27.54	+16.69	+25.38
Third minute of occlusion	-2.99	+24.65	-5.07	+22.47	+5.53	+30.91
First minute after cuff deflation	-11.23	+13.42	-7.77	+14.7	-21.44	+9.47
Second minute after cuff deflation	-2.76	+10.66	-3.44	+11.26	-3.61	+5.86

TABLE 2 Arterial occlusion challenge: Total fluctuations of total blood volume (TBV), oxy- (HbO₂) and deoxy-hemoglobin (Hb) compared to the baseline along with per-minute percentage changes for all healthy volunteers

Time	TBV		HbO ₂		Hb	
	Δ (%)	Total (%)	Δ (%)	Total (%)	Δ (%)	Total (%)
First minute of occlusion	+7.39	+7.39	+5.96	+5.96	+9.11	+9.11
Second minute of occlusion	-2.01	+5.38	+0.09	+6.05	-1.12	+7.99
Third minute of occlusion	+3.97	+9.35	+2.19	+8.24	+6.91	+14.9
First minute after cuff deflation	+0.14	+9.49	+5.44	+13.68	-13.01	+1.89
Second minute after cuff deflation	-0.96	+8.53	-5.47	+8.21	+2.98	+4.87

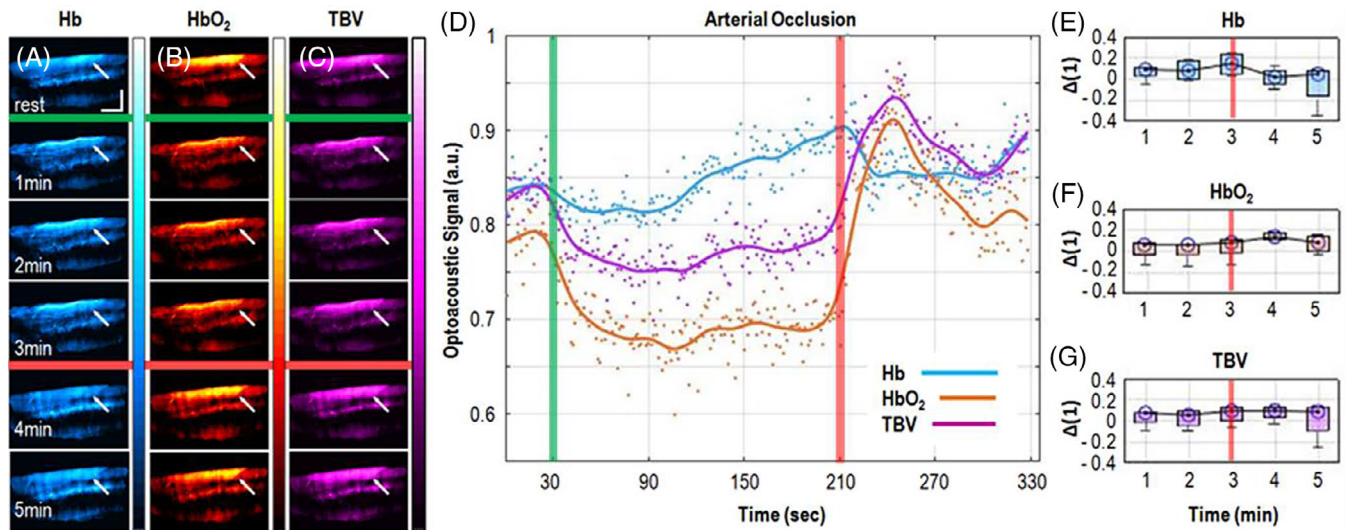


FIGURE 3 Multispectral optoacoustic tomography (MSOT) imaging of the forearm muscle hemodynamics and oxygen kinetics during arterial occlusions. The whole process lasts 5.5 min: 0.5 min of baseline measurement, 3 min of cuff-induced arterial occlusion and 2 min measurement after cuff deflation. Representative image series of A, Deoxy-hemoglobin (Hb)-distribution (MSOT at 750 nm), B, oxy-hemoglobin (HbO₂)-distribution (MSOT at 850 nm) and C, total blood volume (TBV)-distribution (MSOT at 800 nm) within the segmented skeletal muscle area at different time points of the arterial occlusion challenge (Subject 3). The white arrows point to the muscle region where the changes are more prominent. Scale bars: 1 cm. (D) Representative time plot (smoothing splines) of the mean optoacoustic signal for Hb, HbO₂ and TBV within the segmented muscle area over the whole arterial occlusion challenge (Subject 1). Box plot of the mean change of E, Hb, F, HbO₂ and G, TBV optoacoustic signal within the muscle for each minute of the arterial occlusion challenge, with regard to the corresponding baseline value for all (n = 4) subjects. Even if the HbO₂ signal in, F, remains relatively stable during the arterial occlusion, as in a low flow and not in a complete ischemia state, the hyperemic reaction after the cuff deflation is still clear. The green thin stripe corresponds to the time point of cuff inflation. The red thin stripe corresponds to the time point of cuff deflation

average intensities of the optoacoustic signal in the muscle ROI during each minute of the challenge.

3.2 | Arterial occlusion challenge

The MSOT recordings during the arterial occlusion challenge showed a restriction in muscle perfusion and oxygenation with a clear rebound effect after the release of the cuff occlusion or else during the hyperemia period.

As observed, during the arterial occlusion there is an increase in the intramuscular Hb-signal (+14.9% compared to baseline at 3 minutes after cuff inflation) with a decrease (−13.01%) after cuff deflation, reaching a level of only +1.89% above the baseline. On the contrary, the HbO₂-signal remains roughly stable or decreases in selected cases (e.g. Subject 3) during the arterial occlusion and prominently increases during the postocclusive hyperemic period (+13.68% at 1 minute after cuff deflation). Only minor fluctuations are observed for the median value of the corresponding intramuscular TBV-signal over the complete arterial occlusion challenge. The total MSOT readouts for the hemodynamics and oxygen kinetics during the arterial occlusion challenge showed (Table 2):

The aforementioned trends can be inspected visually in Figure 3. Figure 3A depicts representative MSOT images of the Hb-distribution (750 nm) over the examined muscle for each minute of the arterial occlusion challenge (Subject 3). Figure 3B,C shows the MSOT image series for the HbO₂ (at 850 nm) and TBV (at 800 nm) intramuscular distributions of the same subject on a per-minute basis. Figure 3D shows the fluctuations of the mean values of Hb- (blue line), HbO₂- (magenta line) and TBV-signal (orange line) within the muscle region of interest. Figure 3E depicts the statistics of the Hb-levels during the arterial occlusion test for the group of examined healthy volunteers. Furthermore, Figure 3F,G shows the box plots for HbO₂- and TBV-kinetics during the 3-minute arterial occlusions for all (n = 4) subjects. The per-minute median values represent again the change from the baseline for each subject and are extracted from the mean values of optoacoustic signal over the muscle region during each minute of the test.

4 | DISCUSSION

The assessment of peripheral muscle hemodynamics and oxygenation during vascular occlusions is important for

monitoring a spectrum of diseases relating to peripheral vascular function or systemic cardiovascular sufficiency. Different tests exist to assess aspects of insufficient blood supply and oxygenation, including from simple visual observation for signs of cyanosis, pulse oximeter measurements of arterial blood saturation, and blood flow profiling using Doppler ultrasound. Nevertheless, no established clinical test today measures directly the oxygenation and secondary the perfusion of certain organs.

Because the aforementioned techniques, such as the ultrasound, the magnetic resonance and the nuclear medicine techniques, make use of indirect measurements, they fail to meet several critical clinical needs. These could include the objective quantification of PAD severity, the effect of systemic conditions such as heart failure or chronic obstructive pulmonary disease on peripheral muscle oxygen delivery, or even the early detection of septic shock by monitoring peripheral tissue hemodynamics.

By conducting targeted measurements on healthy volunteers, we demonstrate herein the capability of clinical hand-held MSOT to record pathophysiologically expected results during tests of disturbed blood flow with high spatial and temporal resolution and without the need for contrast agents. Thus, by resolving spatial and temporal hemoglobin gradients, MSOT could serve as a novel tool for imaging muscle hemodynamics and oxygenation during several functional challenges, which affect blood flow, such as the venous occlusion as the one developed in venous thrombosis or the arterial occlusion developed in peripheral arterial disease or critical limb ischemia. For example, the arterial occlusion challenge conducted here is a well-established method for the non-invasive assessment of microvascular endothelial dysfunction in soft tissues such as the muscle or the skin: an indicator of increased risk for developing cardiovascular and metabolic disease [23–25].

Our recordings during arterial and venous occlusion challenges showed pathophysiologically expected results, as reported by means of alternative methods for measuring soft tissue hemodynamics and oxygenation [26, 27]. During cuff-induced venous occlusion, a condition simulating CVI or DVT, the cuff pressure (80 mmHg) blocks the venous drainage of the forearm leaving the arterial inflow unaffected and leading to an increase in the forearm volume. MSOT-recorded values showed a clear increase in intramuscular HbO_2 , Hb and TBV within the segmented muscle area. Our results comply with reported measurements conducted by means of other label-free methods, such as the NIRS and the venous occlusion plethysmography (VOP), a method used to estimate the limb blood flow, based on the changes in the limb volume under cuff-induced venous occlusion [28, 29].

However, clinical MSOT is capable of providing not only precise one-dimensional time-series measurements, as usually provided by other methods, but also high-resolution (approximately 250 μm) tomographic images of the muscle tissue with additional spatial maps of perfusion and oxygenation in real-time. Of importance herein is the ability to differentiate depth (up to 3–4 cm) in contrast to diffuse optical methods, due to the higher resolution achieved. This capacity makes MSOT much more accurate than optical imaging or spectroscopy methods, because in MSOT muscle-specific contributions can be quantified based on image guidance. As seen in the morphological images of muscle, optoacoustic imaging can clearly delineate tissue structures, allowing for precisely targeted measurements. This is an important strength over diffuse optical methods characterized by positional uncertainty due to the significant image blurring and the ill-posed nature of the quantitative problem solved.

During cuff-induced arterial occlusion, a condition simulating PAD, the cuff pressure (40 mm Hg above individual's systolic blood pressure, SBP) blocks the arterial inflow and the venous drainage of the forearm leaving essentially unaffected the forearm volume. During arterial occlusion measurements, the MSOT-extracted Hb-value showed an increase, revealing a deoxygenation of the muscle tissue due to complete cessation of the inflow of oxygenated arterial blood. Although arterial occlusion was expected to lead to a prominent decrease in intramuscular HbO_2 for all participants, our results showed a decrease in selected cases (eg, Subject 3) but a roughly steady HbO_2 across the whole cohort. It has been shown in the past that cuff inflation even at pressures significantly higher than the SBP could lead to subtotal arterial occlusion and a state of arterial low flow during the cuff-on period [30]. Even under this condition, it is the abrupt increase of the flow-induced wall shear stress after the cuff deflation which stimulates the vascular endothelium to produce and secrete nitric oxide, a potent vasodilatory molecule that leads to tissue hyperemia [31]. MSOT was capable of detecting and quantifying this phenomenon, showcasing high sensitivity since it can give reliable readouts even under subtotal arterial occlusion where low flow and not total ischemia are present.

Even if MSOT shows great potential for imaging muscle perfusion and oxygenation, it does not come without limitations. Due to light attenuation effects (scattering and absorption) with increasing depth, MSOT is characterized by low penetration (3–4 cm) compared to other clinical imaging modalities. Furthermore, the spectral unmixing of multispectral optoacoustic data is error-prone because of the “spectral coloring” effect or else the deviation of the measured absorption spectrum of a deeplying light absorber (eg, Hb) from its known spectrum

due to light-tissue interactions before the illumination light reaches it. Even if solutions have been presented for preclinical MSOT data [32], this effect hampers the absolute quantification of light absorbers in living tissues and remains a challenging problem for clinical MSOT imaging. To avoid such sources of error, all calculations presented in the current study were performed on raw measured MSOT data.

We presented herein the first, to our knowledge, attempt to record precise tomographic images of intramuscular hemodynamic and oxygenation phenomena during periods of disturbed blood flow. MSOT provided pathophysiologically expected results without the need for injected contrast agents, increasing patient convenience and decreasing costs. Furthermore, MSOT measurements did not require special subject and equipment preparation and may be easily incorporated into daily clinical routine opening up to new possibilities for clinical metabolic imaging of normal or dysfunctional muscle. Our work displays the capacity of MSOT in tracking such phenomena, suggesting it as a research and clinical imaging tool to investigate exercise muscle physiology, peripheral and systemic diseases such as PAD or heart failure, as well as metabolic diseases, such as diabetes mellitus. Subsequent focused studies will advance MSOT towards clinical translation, which will impact objective diagnostics and evaluation of applied pharmacological or interventional therapies.

ACKNOWLEDGMENTS

This project has received funding from the European Research Council (ERC) under the European Union's Horizon 2020 research and innovation program under grant agreement No 694968 (PREMSOT) and was supported by the DZHK (German Centre for Cardiovascular Research) and by the BMBF (German Ministry of Education and Research) and by the Helmholtz Zentrum München, funding program "Physician Scientists for Groundbreaking Projects."

CONFLICTS OF INTEREST

V. N. has stock/stock options in iThera Medical. All other authors have no conflicts of interest to declare.

ORCID

Michail Bariotakis  <https://orcid.org/0000-0002-7624-5675>

REFERENCES

- [1] E. P. Brass, W. R. Hiatt, S. Green, *Vasc. Med.* **2004**, *9*, 293.
- [2] D. C. Poole, D. M. Hirai, S. W. Copp, T. I. Musch, *Am J Physiol Heart Circ Physiol* **2012**, *2012*(302), H1050.
- [3] C. M. Gibson, C. P. Cannon, W. L. Daley, J. T. Dodge, B. Alexander, S. J. Marble, M. C. CH, L. Raymond, T. Fortin, W. K. Poole, E. Braunwald, Group ftTS, *Circulation* **1996**, *93*, 879.
- [4] M. E. Gschwandtner, H. Ehringer, *Vasc. Med.* **2001**, *6*, 169.
- [5] K. Liu, L. E. Chen, A. V. Seaber, G. W. Johnson, J. R. Urbaniak, *J. Orthop. Res.* **1999**, *17*, 88.
- [6] T. Durduran, R. Choe, W. B. Baker, A. G. Yodh, *Rep. Prog. Phys.* **2010**, *73*, 076701.
- [7] T. Hamaoka, K. K. McCully, V. Quaresima, K. Yamamoto, B. Chance, *J. Biomed. Opt.* **2007**, *12*, 062105.
- [8] A. Gibson, H. Dehghani, *Philos. Transact. A Math. Phys. Eng. Sci.* **2009**, *367*, 3055.
- [9] G. Strangman, M. A. Franceschini, D. A. Boas, *Neuroimage* **2003**, *18*, 865.
- [10] D. A. Boas, A. M. Dale, M. A. Franceschini, *Neuroimage* **2004**, *23*(Suppl 1), S275.
- [11] K. J. Kek, R. Kibe, M. Niwayama, N. Kudo, K. Yamamoto, *Opt. Express* **2008**, *16*, 18173.
- [12] A. Karlas, J. Reber, G. Diot, D. Bozhko, M. Anastasopoulou, T. Ibrahim, M. Schwaiger, F. Hyafil, V. Ntziachristos, *Biomed. Opt. Express* **2017**, *8*, 3395.
- [13] A. Karlas, N. A. Fasoula, K. Paul-Yuan, J. Reber, M. Kallmayer, D. Bozhko, M. Seeger, H. H. Eckstein, M. Wildgruber, V. Ntziachristos, *Photoacoustics*. **2019**, *14*, 19.
- [14] M. Masthoff, A. Helfen, J. Claussen, A. Karlas, N. A. Markwardt, V. Ntziachristos, M. Eisenblatter, M. Wildgruber, *JAMA dermatology* **2018**, *154*(12), 1457–1462.
- [15] G. Diot, S. Metz, A. Noske, E. Liapis, B. Schroeder, S. V. Ovsepian, R. Meier, E. Rummeny, V. Ntziachristos, *Clin Cancer Res* **2017**, *23*, 6912.
- [16] M. Masthoff, A. Helfen, J. Claussen, W. Roll, A. Karlas, H. Becker, G. Gabriels, J. Riess, W. Heindel, M. Schafers, V. Ntziachristos, M. Eisenblatter, U. Gerth, M. Wildgruber, *J. Biophotonics* **2018**, *11*, e201800155.
- [17] F. Knieling, C. Neufert, A. Hartmann, J. Claussen, A. Urich, C. Egger, M. Vetter, S. Fischer, L. Pfeifer, A. Hagel, C. Kielisch, R. S. Gortz, D. Wildner, M. Engel, J. Rother, W. Uter, J. Siebler, R. Atreya, W. Rascher, D. Strobel, M. F. Neurath, M. J. Waldner, *N. Engl. J. Med.* **2017**, *376*, 1292.
- [18] J. Reber, M. Willershäuser, A. Karlas, K. Paul-Yuan, G. Diot, D. Franz, T. Fromme, S. V. Ovsepian, N. Bézière, E. Dubikovskaya, D. C. Karampinos, C. Holzapfel, H. Hauner, M. Klingenspor, V. Ntziachristos, *Cell. Metab.* **2018**, *27*, 689.
- [19] G. Diot, A. Dima, V. Ntziachristos, *Opt. Lett.* **2015**, *40*, 1496.
- [20] America. TLlo. American national standards for the safe use of lasers. *ANSI Z136.1*. 2000.
- [21] A. Rosenthal, V. Ntziachristos, D. Razansky, *Med. Phys.* **2011**, *38*, 4285.
- [22] T. F. Chan, L. A. Vese, *IEEE Transact Image Proces.* **2001**, *10*, 266.
- [23] P. O. Bonetti, L. O. Lerman, A. Lerman, *Arterioscler. Thromb. Vasc. Biol.* **2003**, *23*, 168.
- [24] F. Cosentino, S. Rubattu, C. Savoia, V. Venturelli, E. Pagannonne, M. Volpe, *J. Cardiovasc. Pharmacol.* **2001**, *38* (Suppl 2), S75.
- [25] Y. Shi, P. M. Vanhoutte, *J. Diabetes* **2017**, *9*, 434.
- [26] F. Liao, S. Burns, Y. K. Jan, *J. Tissue Viability* **2013**, *22*, 25.

- [27] J. L. Cracowski, C. T. Minson, M. Salvat-Melis, J. R. Halliwill, *Trends Pharmacol. Sci.* **2006**, *27*, 503.
- [28] T. J. Cross, S. Sabapathy, *Clin. Physiol. Funct. Imaging* **2017**, *37*, 293.
- [29] I. B. Wilkinson, D. J. Webb, *Br. J. Clin. Pharmacol.* **2001**, *52*, 631.
- [30] J. R. Spiro, J. E. Digby, G. Ghimire, M. Mason, A. G. Mitchell, C. Ilsley, A. Donald, M. C. Dalby, R. K. Kharbanda, *Eur Heart J* **2011**, *32*, 856.
- [31] M. C. Corretti, T. J. Anderson, E. J. Benjamin, D. Celermajer, F. Charbonneau, M. A. Creager, J. Deanfield, H. Drexler, M. Gerhard-Herman, D. Herrington, P. Vallance, J. Vita, R. Vogel, *J. Am. Coll. Cardiol.* **2002**, *39*, 257.
- [32] S. Tzoumas, A. Nunes, I. Olefir, S. Stangl, P. Symvoulidis, S. Glasl, C. Bayer, G. Multhoff, V. Ntziachristos, *Nat. Commun.* **2016**, *7*, 12121.

How to cite this article: Karlas A, Kallmayer M, Fasoula N-A, et al. Multispectral optoacoustic tomography of muscle perfusion and oxygenation under arterial and venous occlusion: A human pilot study. *J. Biophotonics*. 2020;13:e201960169. <https://doi.org/10.1002/jbio.201960169>